IEEE Access
Multidisciplinary | Rapid Review | Open Access Journal

Received December 10, 2020, accepted January 3, 2021, date of publication January 8, 2021, date of current version January 14, 2021.

Digital Object Identifier 10.1109/ACCESS.2021.3049880

An Open Source Patient Simulator for Design and Evaluation of Computer Based Multiple Drug Dosing Control for Anesthetic and Hemodynamic Variables

CLARA M. IONESCU[1], (Senior Member, IEEE), MARTINE NECKEBROEK[2], MIHAELA GHITA[1], (Graduate Student Member, IEEE), AND DANA COPOT[1], (Member, IEEE)

[1]Dynamical Systems and Control Research Group, Department of Electromechanical, Systems and Metal Engineering, Ghent University, 9052 Ghent, Belgium
[2]Department of Anesthesia, Ghent University Hospital, 9000 Ghent, Belgium

Corresponding author: Clara M. Ionescu (claramihaela.ionescu@ugent.be)

This work was supported by the Flemish Research Foundation (FWO) under Project 026514N and Project 1501517N. The work of Mihaela Ghita was supported by the FWO Doctoral Fellowship under Grant 1184220N. The work of Dana Copot was supported by the FWO Postdoctoral Fellowship under Grant 12X6819N.

ABSTRACT We are witnessing a notable rise in the translational use of information technology and control systems engineering tools in clinical practice. This paper empowers the computer based drug dosing optimization of general anesthesia management by means of multiple variables for patient state stabilization. The patient simulator platform is designed through an interdisciplinary combination of medical, clinical practice and systems engineering expertise gathered in the last decades by our team. The result is an open source patient simulator in Matlab/Simulink from Mathworks(R). Simulator features include complex synergic and antagonistic interaction aspects between general anesthesia and hemodynamic stabilization variables. The anesthetic system includes the hypnosis, analgesia and neuromuscular blockade states, while the hemodynamic system includes the cardiac output and mean arterial pressure. Nociceptor stimulation is also described and acts as a disturbance together with predefined surgery profiles from a translation into signal form of most commonly encountered events in clinical practice. A broad population set of pharmacokinetic and pharmacodynamic (PKPD) variables are available for the user to describe both intra- and inter-patient variability. This simulator has some unique features, such as: i) additional bolus administration from anesthesiologist, ii) variable time-delays introduced by data window averaging when poor signal quality is detected, iii) drug trapping from heterogeneous tissue diffusion in high body mass index patients. We successfully reproduced the clinical expected effects of various drugs interacting among the anesthetic and hemodynamic states. Our work is uniquely defined in current state of the art and first of its kind for this application of dose management problem in anesthesia. This simulator provides the research community with accessible tools to allow a systematic design, evaluation and comparison of various control algorithms for multi-drug dosing optimization objectives in anesthesia.

INDEX TERMS Computer based drug management, optimal drug dosing, depth of anesthesia, hemodynamic stabilization, nociceptor stimulation, dose effect response, surface models, inter-patient variability, drug synergy, drug trapping, variable delay, anomalous diffusion, predictive control, adaptive control.

I. INTRODUCTION

Progress in medical science, healthcare and clinical practice is often paired with information technology tools and control expertise of computer based monitoring. It allows data monitoring and management, offers decision-making support and provides patient stabilization during surgical procedures, intensive care and recovery/rehabilitation periods. Results in both simulation and clinical trial testing provide evidence that computer based control of anesthesia outperforms to

The associate editor coordinating the review of this manuscript and approving it for publication was Salman Ahmed.

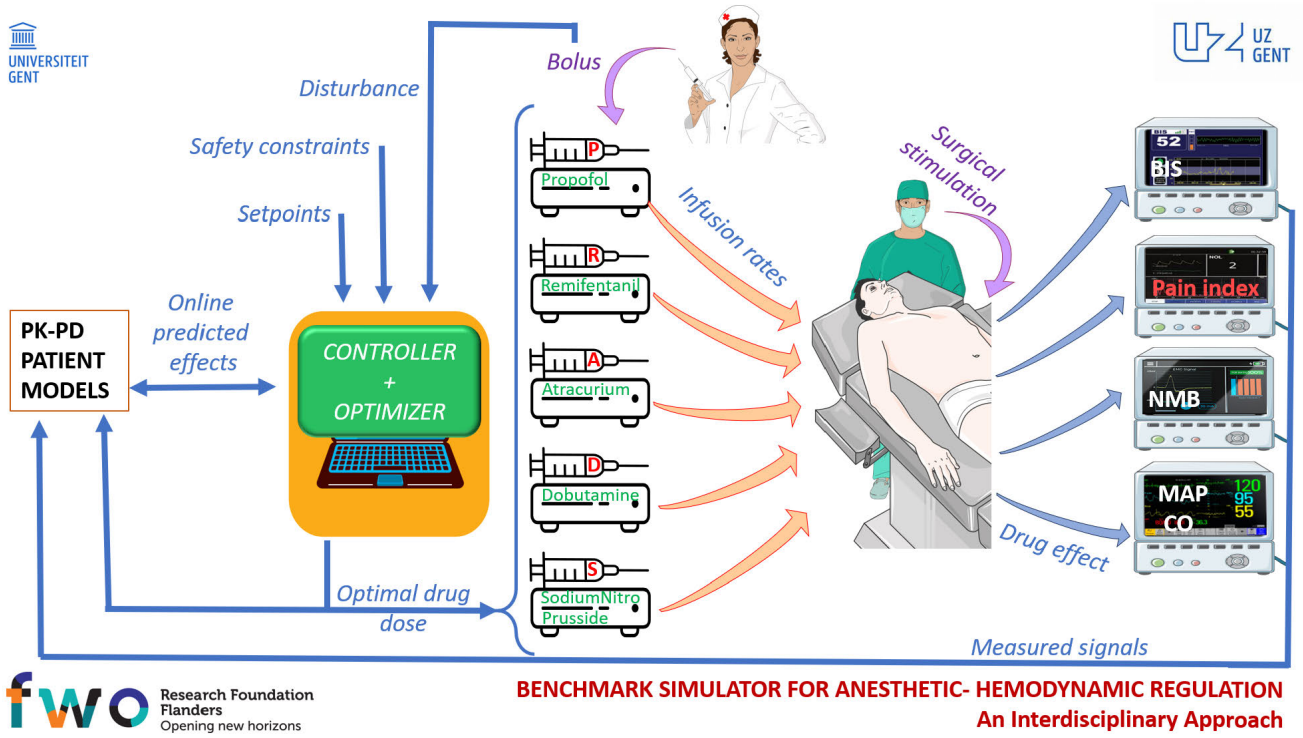

FIGURE 1. Conceptual representation of the sedation and hemodynamic systems involved in the balancing act of optimizing general anesthesia.

manual dosing techniques [1]–[6]. Based on these incentives, the systems and control engineering community steps forward towards optimizing co-administration of drug cocktails to stabilize patient variables in a synergic context of interacting vital sign profiles [7]. Ensuring clinical relevant progress is a challenging task which requires a systematic comparison of algorithms, thereby demanding availability of adequate simulation tools before transferring results to clinical practice for testing.

Notable closed loop simulations and closed loop clinical data for regulating depth of anesthesia using computer control algorithms have been published recently [8]–[10]. We are at the very beginning of what we call - a new era of personalized medicine - enabled by advances in computer technology and powerful information technology processing tools, in which artificial intelligence tools are prevalent [11]–[14]. In an effort to provide the cross-disciplinary community with suitable and accessible tools for systematic analysis of pros- and cons- of various control algorithms, a patient simulator has been programmed in Matlab/Simulink from MathWorks(R) software platform. This is an open source patient simulator, where the community can set, add and modify its components as know-how and insight become available.

This paper describes the various components of the patient simulator in general anesthesia. It gives an overview of the embedded features to closely mimic the clinical and physiological responses to various drug dosing schemes. The authors have used their 15 years experience in the topic combined with survey of literature reports to distill, transfer and program in an understandable and accessible manner the afferent complex patient dynamics. Where available, clinical data has been curated and used in the simulator parameters to better mimic clinical practice. Two main dynamic interactive systems are described: i) depth of anesthesia and ii) hemodynamic system. The patient simulator is an open source file archive in which the user can change models, conditions, set values and add control algorithms for the final aim to maintain a balance of all variables within clinically safe intervals.

Our objective is to encourage the community to work in a systematic and fair-to-compare context while developing computer based control of multi-drug anesthesia regulatory problems. The novelty is the provision of the patient simulator as to date no such tools has been previously reported in literature for the systems and control community. The originality of the approach is the inclusion of synergy effects, antagonist effects, patient variability, clinical value intervals, nociceptor stimulation disturbance, drug trapping models and co-simulation of anesthestic and hemodynamic states along with their complex interactions. The conceptual representation of the various synergic and antagonistic interactions between sedation and hemodynamic systems is given in Fig. 1.

The paper is organized as follows. The second section starts with providing the reader with a generic representation of compartmental models for PKPD patient model. Following sub-sections specify the PKPD models for anesthesia and

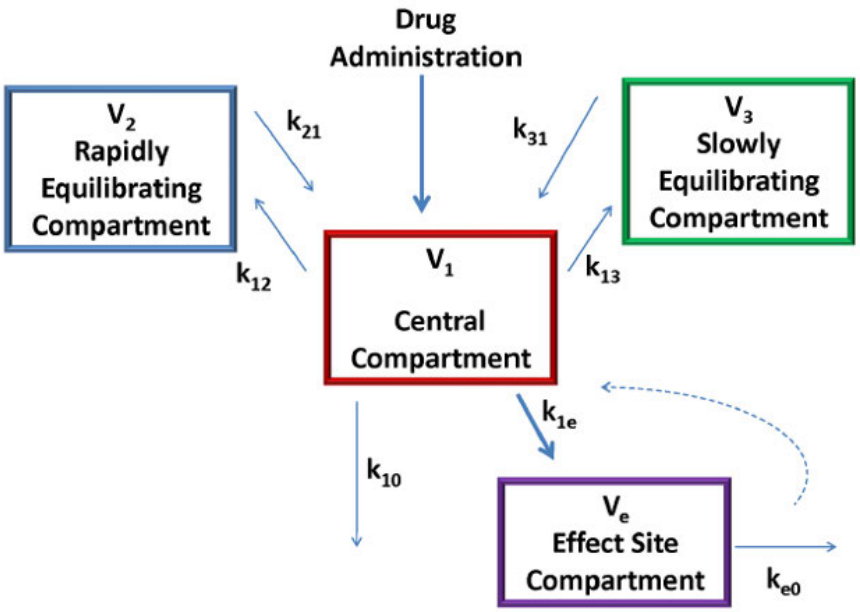

FIGURE 2. Compartmental scheme of the pharmacokinetic model for one drug.

hemodynamic systems along with their complex dynamic interactions (synergic and antagonistic) and patient database values. The second sections ends with the disturbance signal translated from clinical events during surgery and its nociceptor stimulation dynamic model, including possibility to add bolus profiles. The third section provides an overview of simulator features embedded in this initial version. The fourth section presents the open loop results depicting the synergic and antagonist reactions caused by various drug dosing profiles within the simulator and gives an overview on the interval variability in patient's dynamic response. The fifth section provides a discussion into the opportunities and the potential research challenges enabled by this simulation tool and provides some perspectives for the simulator use. A conclusion section summarizes the main outcome of the work and poses some research questions.

II. MATERIALS AND METHODS

A. COMPARTMENTAL MODEL FORMS

Compartmental models are often used to predict/suggest the optimal dosage of drugs and they are at the backbone of target controlled infusion management systems in clinical practice [15]. Generically, a three-compartment pharmacokinetic model describes the fast acting compartment (blood) with two additional compartments representing slower acting tissue volumes (muscle and fat), as in Fig. 2 and represented by the set of differential equations:

$$\begin{aligned}\dot{x}_1(t) &= -(k_{10}+k_{12}+k_{13})x_1(t)+k_{21}x_2(t)+k_{31}x_3(t)\\ \dot{x}_2(t) &= k_{12}x_1(t)-k_{21}x_2(t)\\ \dot{x}_3(t) &= k_{13}x_1(t)-k_{31}x_3(t)\end{aligned} \tag{1}$$

where x_1 (mg/ml) is the concentration in the fast compartment, while x_2 (mg/ml) and x_3 (mg/ml) denote the concentrations of drug in slow compartments. The constants k_{ij} $(i, j = 1, 2, 3, i \neq j)$ represent the drug amount transfer rate from the i-th compartment to the j-th compartment. A hypothetical compartment representing the transport/mixing dynamics of drug to the effect location is added and denoting the effect site concentration x_e:

$$\dot{x}_e(t) = -k_{e0}x_e(t)+k_{1e}x_1(t) \tag{2}$$

where the constant k_{e0} represents the drug metabolic rate. Intravenous drug dosing will be added in the first compartment (blood, x_1) as an extra variable, usually denoted as a manipulated input by $u(t)/V_1$ and has the meaning of drug infusion rate (mg/ml/min). In matrix form this can be written as:

$$\begin{bmatrix}\dot{x}_1\\ \dot{x}_2\\ \dot{x}_3\\ \dot{x}_e\end{bmatrix} = \begin{bmatrix}-(k_{10}+k_{12}+k_{13}) & k_{21} & k_{31} & 0\\ k_{12} & -k_{21} & 0 & 0\\ k_{13} & 0 & -k_{31} & 0\\ k_{1e} & 0 & 0 & -k_{e0}\end{bmatrix}\begin{bmatrix}x_1\\ x_2\\ x_3\\ x_e\end{bmatrix} + \begin{bmatrix}1\\ 0\\ 0\\ 0\end{bmatrix}u(t) \tag{3}$$

which delivers the states x_i denoting the concentration in volume compartments and the manipulated variable $u(t)$ denoting input drug infusion rate. The drug metabolic rate is calculated in function of lean body mass (LBM) as:

$$LBM = 1.1 * weight - 128 * (weight/height)^2 \tag{4}$$

for male patients and calculated as:

$$LBM = 1.07 * weight - 148 * (weight/height)^2 \tag{5}$$

for female patients. The units for height and weight are *cm* and respectively *kg*.

The equivalent 4th-order linear transfer function model is obtained using the formula $G(s) = C(sI - A)^{-1}B + D$, with the following matrices:

$$\begin{aligned} A &= \begin{bmatrix} -(k_{10}+k_{12}+k_{13}) & k_{21} & k_{31} & 0 \\ k_{12} & -k_{21} & 0 & 0 \\ k_{13} & 0 & -k_{31} & 0 \\ k_{1e} & 0 & 0 & -k_{e0} \end{bmatrix} \\ B &= \begin{bmatrix} 1 \\ 0 \\ 0 \\ 0 \end{bmatrix} \\ C &= \begin{bmatrix} 0 & 0 & 0 & 1 \end{bmatrix} \\ D &= 0 \end{aligned} \tag{6}$$

The dose-effect response in the PD model is represented by a nonlinear Hill equation, which relates values of the drug concentration profiles with values of its effect. When single drugs are modeled, the relationship is given by the generic formula:

$$E = E_0 - \frac{E_{max} \cdot x_e^{\gamma}}{C_{50}^{\gamma} + x_e^{\gamma}} \tag{7}$$

where E [%] denotes the (predicted) effect of the drug, x_e is the effect site concentration of the drug at time t, C_{50} is the concentration needed to obtain 50% of the maximum effect E_{max}[%] and γ [-] the Hill-coefficient of sigmoidicity [16], [17].

B. DEPTH OF ANESTHESIA SYSTEM

General anesthesia is a broad term encompassing the use of drugs to induce and maintain three states during surgery: hypnosis (depth of unconsciousness), analgesia (absence of pain) and areflexia (neuromuscular blockade). Measuring the level of hypnosis is achieved by monitoring electroencephalogram (EEG) signals to determine the depth of anesthesia, usually via processed variables such as Bispectral Index (BIS). Other measurable clinical variables have been summarized in [18]–[21] for both hypnosis and analgesia.

The intensity of a surgical stimulation during surgery, hemodynamic effects of the drugs, under-dosing due to equipment failure and overdosing due to inappropriate titration of the hypnotic components, among other factors, often result in imbalances between the amount of anesthetic required and the amount of anesthetic delivered. Inappropriate anesthetic delivery can have severe consequences. If not enough anesthetic is delivered, the patient can remain conscious (but paralyzed) during surgery which causes both trauma and anxiety. Too much anesthetic may have detrimental long term effects on the patient and prolongued recovery times in critical care unit.

In this simulator we use Propofol, Remifentanil and Atracurium as manipulated variables for control to induce hypnosis, analgesia and neuromuscular blockade respectively. Their effect are monitored/controlled variables of BIS (Bispectral Index), RASS (Ramsay Agitation Score) and EMG (electromyogram) values, respectively. These drugs have been acclaimed numerous times in both clinical and biomedical engineering literature for being suitable in a computerized closed loop control paradigm for their fast onset and recovery times [18], [22].

The PKPD model for Propofol absorption and effect is used here [23], [24]. This is a three-compartmental model in form of (1) denoting fast acting (blood) and slow acting (muscle and fat) volumes of drug distribution areas followed by a transport first order compartment with nonlinear sigmoid relationship for dose-effect response. The same PKPD model structure is used for the Remifentanil drug characterization.

Propofol pharmacokinetic model parameters are calculated using the set of equations [25]:

$$\begin{aligned} k_{10} &= \frac{C_{l1}}{V_1}\,[1/min];\ k_{12} = \frac{C_{l2}}{V_1}\,[1/min]; \\ k_{13} &= \frac{C_{l3}}{V_1}\,[1/min];\ k_{21} = \frac{C_{l2}}{V_2}\,[1/min]; \\ k_{31} &= \frac{C_{l3}}{V_3}\,[1/min];\ k_{e0} = k_{1e} = 0.456\,[1/min] \\ V_1 &= 4.27[l];\ V_3 = 238[l] \\ V_2 &= 18.9 - 0.391(age - 53);\,[l] \\ C_{l1} &= 1.89 + 0.0456(weight - 77) - 0.0681(lbm - 59) \\ &\quad + 0.0264(height - 177)\,[l/min] \\ C_{l2} &= 1.29 - 0.024(age - 53)\,[l/min]; \\ C_{l3} &= 0.836\,[l/min] \end{aligned} \tag{8}$$

where the constants V_i ($i = 1, 2, 3$) denote the volume of the i-th compartment, and their clearance rates C_{li} respectively. In model form (1) the extra input in the first compartment is denoted as $u_P(t)/V_1$ for Propofol infusion rates (mg /ml/min). Equivalent transfer function models have been proposed in [26].

In a similar pharmacokinetic model representation as (1), the Remifentanil model parameters are calculated using the set of equations [27]:

$$\begin{aligned} k_{10} &= \frac{C_{l1}}{V_1}\,[1/min]\ k_{12} = \frac{C_{l2}}{V_1}\,[1/min] \\ k_{13} &= \frac{C_{l3}}{V_1}\,[1/min]\ k_{21} = \frac{C_{l2}}{V_2}\,[1/min] \\ k_{31} &= \frac{C_{l3}}{V_3}\,[1/min]\ k_{e0} = 0.595 - 0.007(age - 40)\,[1/min] \\ V_1 &= 5.1 - 0.0201(age - 40) + 0.072(lbm - 55)\,[l]; \\ V_2 &= 9.82 - 0.0811(age - 40) + 0.108(lbm - 55)\,[l] \\ V_3 &= 5.42\,[l] \\ C_{l1} &= 2.6 + 0.0162(age - 40) + 0.0191(lbm - 55)\,[l/min]; \\ C_{l2} &= 2.05 - 0.0301(age - 40)\,[l/min] \\ C_{l3} &= 0.076 - 0.00113(age - 40)\,[l/min] \end{aligned} \tag{9}$$

In model form (1) the extra input in the first compartment is denoted as $u_R(t)/V_1$ for Remifentanil infusion rates (μ g /ml/min), where the constants V_i ($i = 1, 2, 3$) denote the volume of the i-th compartment, and their clearance rates C_{li} respectively.

Given our past expertise and studies in cooperation with Ghent University Hospital Belgium and University Medical Center Groningen The Netherlands, a database of patient profiles has been artificially created to mimic as close as possible reality. The details for the pharmacokinetic models are given in Table 1 [8], [28], with PD model values for Propofol listed in Table 1, and generic PD model values for Remifentanil to BIS given as C_{50}=11.4 [ng/ml] and γ=2.5 as from [27].

TABLE 1. Representative Patient Database for Propofol-to-BIS with pharmacokinetic Model Biometric Values and PD Model Sensitivity Values.

Index	Age	Height	Weight	C_{50}	γ
-	(yrs)	(cm)	(kg)	(mg/ml)	-
1	74	164	88	2.5	3
2	67	161	69	4.6	2
3	75	176	101	5	1.6
4	69	173	97	1.8	2.5
5	45	171	64	6.8	1.78
6	57	182	80	2.7	2.8
7	74	155	55	1.7	3.5
8	71	172	78	7.8	2.9
9	65	176	77	2.9	1.88
10	72	192	73	3.9	3.1
11	69	168	84	2.3	3.1
12	60	190	92	4.8	2.1
13	61	177	81	2.5	3
14	54	173	86	2.5	3
15	71	172	83	4.3	1.9
16	53	186	114	2.7	1.6
17	72	162	87	4.5	2.9
18	61	182	93	2.7	1.78
19	70	167	77	6.8	3.1
20	69	168	82	9.8	1.6
21	69	158	81	3.2	2.1
22	60	165	85	5.1	2.51
23	70	173	69	3.67	3.1
24	56	186	99	5.8	2.3

Fig. 3 depicts relation (7) for several patients selected from Table 1, i.e. for significant variations in the values of γ and C_{50}. One may observe the difference in response for the same input of drug bolus. Hence, this figure gives an insight on the amount of inter-patient variability one may expect in practice. Patients a (respectively patient 9 from table 1) and c (respectively patient 3 from table 1) need a high effect site concentration before they start to react, i.e. effect starts to decrease. Patient a has a strong sensitivity to the drug after this minimum concentration of x_e, and it decreases very fast to 0. Patient c has a less sensitivity to the drug so it reacts slower. Finally patient b (respectively patient 6 from table 1) requires less amount of drug infusion before it reacts, but the effect is extremely slow. Hence, each patient's sensitivity to the drug is strongly influenced by the γ and C_{50} parameters. Analysis has been provided in [29], [30].

If the Hill curve is normalized with values between 0% (full drug effect) and 100% (no drug effect), one obtains for

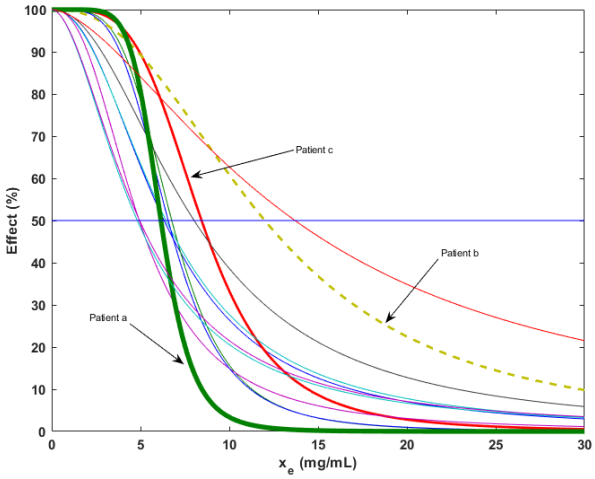

FIGURE 3. Dose-to-effect (Hill) curve for several patients illustrating the great inter-patient variability among their hypnosis response effect.

a given γ value and for a given x_e concentration a line for the PD model of the patient. However, the sensitivity of the patient to the drug is also changing during treatment, i.e. the intra-patient variability concept, hence the slope of the line might vary. The patient sensitivity has been extensively analysed from the view point of control feasibility and reported in [31]. The study indicated a gain variation of up to 15-fold values and concluded that adaptation of controller parameters is necessary to ensure converge to steady state in closed loop dosing context. Adaptation of the PD model values from real time data during anesthesia has been proposed in a computationally efficient recursive method in [32].

There is a synergic effect when using Remifentanil in combination with Propofol, reducing the Propofol concentration for loss of consciousness by 25% and hence minimising the risk of over-dosages [33]. The combined effect of two drugs is then a 3D nonlinear surface. When surface models are used to characterize synergic effects among drugs, the effect drug concentrations x_e are normalized to their potency, i.e. to their corresponding half effect concentration C_{50}. Generally, the combined effect E of two drugs U_A and U_B is considered as a new drug, and expressed as a Hill curve dose-response relationship 3D surface:

$$E = \frac{I^{\gamma}}{1 + I^{\gamma}} \tag{10}$$

with I denoting the interaction term

$$I = \bar{U}_A + \bar{U}_B + \sigma \bar{U}_A \cdot \bar{U}_B \tag{11}$$

with $\bar{U}_A = \frac{U_A}{C_{50A}}$ and $\bar{U}_B = \frac{U_B}{C_{50B}}$ the normalized drug effect concentrations and C_{50} the concentrations at half effect (50%). The term σ denotes the slope sigmoidicity of the Hill surface, which indicates a patient drug responsiveness or drug resistance. The term σ denotes the amount of synergy present between the drugs. In the limits, when either one drug is used, the isobole response has values 0 to 1. If (10) is preceded by a maximum effect coefficient E_{max}, usually

from 0% to 100% efficacy, then the effect is expressed in percent. An example of such surface response for Propofol and Remifentanil is given in Fig. 4, with values for $\sigma = 0.2$, $\gamma = 10$, $C_{50} = 3.5$ [mg/ml] for Propofol and $C_{50} = 4.5$ [μ g/ml]for Remifentanil.

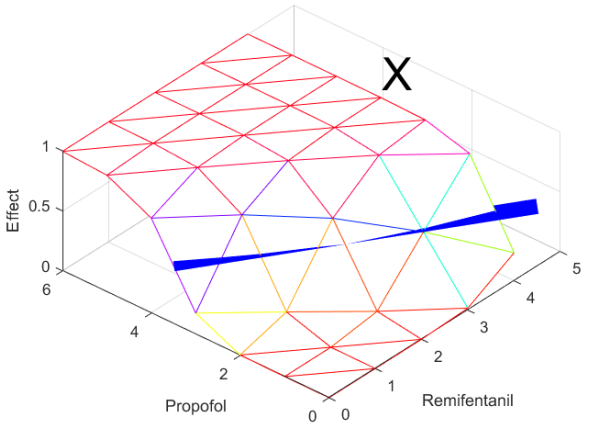

FIGURE 4. BIS interaction surface Propofol and Remifentanil. The "X" marks the population averaged C_{50} values with full effect (1), and the blue line crosses the surface at half -effect response (0.5).

In Fig. 4 one may observe that the half-effect crossing the surface is a line, hence the nonlinearity in the Hill surface is no longer present during maintenance of the anesthetic state. As the setpoint for BIS lies typically between (40,60), the surface is relatively linear and adaptation of the curve through identification to patient response is much simplified in this case. A discussion along with clinical values has been provided in [30], [31].

The independent relation of Remifentanil on the Ramsay Agitation and Sedation Score (RASS) is modelled as:

$$RASS = \frac{1}{k_1 \cdot x_e + k_0} \cdot \frac{-2}{s+2} \tag{12}$$

with $k_1 = k_0 = 0.81$ [34].

The Atracurium PKPD model developed by Weatherley *et al.* [35] can be treated as a two-compartmental pharmacokinetic model and a PD model including a second-order function and nonlinear Hill equation in series. The Atracurium pharmacokinetic model is given by:

$$\begin{aligned} \dot{x}_1 &= -\lambda_1 x_1(t) + a_1 u(t) \\ \dot{x}_2 &= -\lambda_2 x_2(t) + a_2 u(t) \\ C_p &= x_1(t) + x_2(t) \end{aligned} \tag{13}$$

where x_i ($i = 1, 2$) denotes the state variables and a_1, a_2 [kg/ml], k_1, k_2 [kg/min] are the patient-dependent parameters. The drug infusion rate $u(t)$ [μg/kg/min] is the input of this pharmacokinetic model, and the plasma concentration $C_p(t)$ [μg/ml] is the output of this pharmacokinetic model. The Atracurium PD model is described as a cascade of a second-order function and a nonlinear term, and it is formulated as:

$$\dot{C} = -\lambda C(t) + C_p(t)$$

$$\begin{aligned} \dot{x}_e &= -\frac{1}{\tau} x_e(t) + \frac{1}{\tau} C(t) \\ r(t) &= \frac{100 \cdot C_{50}^{\gamma}}{C_{50}^{\lambda} + x_e^{\lambda}(t)} \end{aligned} \tag{14}$$

where x_e(t) is the drug concentration of the effect compartment, $C(t)$ is an intermediate variable, and $r(t)$ [%] is the reflection of NMB level. The variables λ, τ [min], C_{50} [μg/ml] and c [-] are patient-independent parameters. Finally, in the entire Atracurium PKPD model, the parameters a_i ($i = 1, 2$), λ_i ($i = 1, 2$), λ, τ, C_{50} are the patient-response specific parameters.

From [36], the parameters k_1, k_2, k_3 and C_{50} are assumed to be known. Only α and γ remain to be identified, and Table 2 contains the initial values that represent the mean values for the population. The model is described by:

$$\begin{aligned} NMB &= \frac{k_1 \cdot k_2 \cdot k_3 \cdot \alpha^3}{(s + k_1 \cdot \alpha)(s + k_2 \cdot \alpha)(s + k_3 \cdot \alpha)} \\ E &= E_{max} \cdot \frac{C_{50}^{\gamma}}{NMB^{\gamma} + C_{50}^{\gamma}} \end{aligned} \tag{15}$$

TABLE 2. Parameters of the PKPD model for neuromuscular blockade controlled with Atracurium.

k_1	k_2	k_3	C_{50}	α	γ
1	4	10	3.2425	0.0374	2.667

In some clinical studies, the EMG has been measured in patients and considered an index for determining the level of neuromuscular blockade. The effect of Remifentanil on the EMG values has been provided in [37], [38]:

$$EMG = \frac{100 \cdot x_e}{3.4 \cdot x_e + 0.0063} \tag{16}$$

where x_e is the effect site Remifentanil concentration.

C. HEMODYNAMIC SYSTEM

For all patients (but essentially in cardiac patients), the mean arterial pressure (MAP) and the cardiac output (CO) are critical variables [39]. These are maintained in the desired range by administration of Sodium Nitroprusside (SNP) and Dopamine (DP). In clinical practice, Dobutamine (DB) is also used for patients under general anesthesia due to its inotropic actions. The pharmacokinetic of DB following intravenuous administration is described by a one-compartment model with a first order plus dead time elimination rate [18], [40]. This model is analogous to the DP pharmacokinetic model and implemented in the simulator. Since its discovery in 1975, DB has been used off-label for treatment of hemodynamic insufficiency in newborn and children [41], [42]. In this paper we used the DP model, but both DP and DB pharmacokinetic models are available in the simulator. Computer based control of hemodynamic variables was established in the early 90s [11], [43], [44] and found to significantly depend on the anesthesia levels, leading to combined hemodynamic and anesthetic optimization studies [9], [45], [46].

There is evidence to support the claim that sedative and hypnotic drugs affects negatively MAP values [47]. The effect of Remifentanil on MAP is described by:

$$MAP = \frac{-1}{k_1 \cdot x_e + k_0}$$
$$E = E_{max} \cdot \frac{MAP^{\gamma}}{MAP^{\gamma} + C_{50}^{\gamma}} \quad (17)$$

The antagonistic effects of Dopamine and Sodium Nitroprusside on the Cardiac Output and Mean Arterial Pressure are modelled as a 2×2 multivariable system with first order plus dead time approximated transfer function models:

$$\begin{bmatrix} CO \\ MAP \end{bmatrix} = \begin{bmatrix} \frac{K_{11}.e^{-T_{11}s}}{1+\tau_{11}s} & \frac{K_{21}.e^{-T_{21}s}}{1+\tau_{21}s} \\ \frac{K_{12}.e^{-T_{12}s}}{1+\tau_{12}s} & \frac{K_{22}.e^{-T_{22}s}}{1+\tau_{22}s} \end{bmatrix} \begin{bmatrix} DP \\ SNP \end{bmatrix} \quad (18)$$

The parameter intervals for the model (17) are given in table 3 as from [48].

TABLE 3. Interval parameters for the hemodynamic model.

Parameter	Typical	Range	Units
K_{11}	5	1-12	ml/μg
τ_{11}	300	70-600	s
T_{11}	60	15-60	s
K_{12}	3	0-9	mmHg.kg.min/μg
τ_{12}	40	30-60	s
T_{12}	60	15-60	s
K_{21}	12	-15-25	ml/μg
τ_{21}	150	70-600	s
T_{21}	50	15-60	s
K_{22}	-15	-50-(-1)	mmHg.kg.min/μg
τ_{22}	40	30-60	s
T_{22}	50	15-60	s

D. DISTURBANCE AND NOCICEPTION STIMULATION

Literature presents a disturbance signal mimicking surgical stimulation profile [49], as depicted in Fig. 5. Each segment corresponds in order, with the following events: intubation; surgical incision followed by a period of no surgical stimulation (i.e. waiting for pathology result); an abrupt stimulus after a period of low level stimulation; onset of a continuous normal surgical stimulation; short-lasting, larger stimulation within the surgical period; and withdrawal of stimulation during the closing period. For the controller-based regulation protocol, the disturbance signal is not known in advance, and thus enters the system through the feedback loop information flow.

When surgical stimulation is present in the overall system, a nociceptor stimulation occurs. A recently developed method, device and model has been presented in [50], based on a physiological model of pain using fractional order tools reviewed in [51]. A simplified model of the nociceptor pathway is described by the following transfer function model:

$$K \cdot \frac{(s^2 + z_1 s + z_2)(s^2 + z_3 s + z_4)(s^2 + z_5 s + z_6)}{(s^2 + p_1 s + p_2)(s^2 + p_3 s + p_4)(s^2 + p_5 s + p_6)} \quad (19)$$

TABLE 4. Parameter values of the nociceptor pathway model.

i	1	2	3	4	5	6
z_i	$0.6 * 150$	150^2	$0.16 * 165$	165^2	$0.2 * 155$	155^2
p_i	$0.44 * 149$	149^2	$0.3 * 163$	163^2	$0.2 * 155$	155^2
K	2					

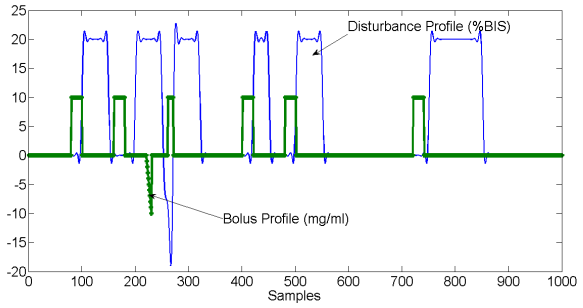

FIGURE 5. The filtered nociceptor stimulation profile and additional signal used for bolus infusion as anticipatory action of the anesthesiologist to incoming disturbance profile. To obtain the clinical effect, these disturbance signal has to be added to the simulated BIS values and the bolus profile has to be added in the fast acting compartment (blood) in (1) with values from (8).

The surgical stimulation profile is then filtered through this model and it is a disturbance at the output of the hypnotic state, i.e. added to the BIS value given by the Hill equation of the PD model of hypnosis.

When the protocol is enhanced with the manual intervention of the anaesthesiologist, an additional input signal is delivered to the system. This additional input signal in form of a bolus is also depicted in Fig. 5 along with the disturbance signal, where one may recognize the anticipatory action of the anaesthesiologist to compensate in part the expected disturbance profile.

III. FEATURES OVERVIEW

There are 5 possible manipulated variables (drug dosing rates) and 5 direct controlled variables (outputs), along with numerous interaction effects.

The direct cause-effect models include:

- Propofol drug rate to hypnotic state evaluated with BIS variable;
- Remifentanil drug rate to analgesic state evaluated with RASS variable;
- Rocuronium/Atracurium drug rate to neuromuscular blockade state evaluated with NMB variable;
- Dopamine(DP)/Dobutamine(DB) drug rate to cardiac output state evaluated with CO variable;
- Sodium Nitroprusside drug rate to mean arterial pressure state evaluated with MAP variable.

The interaction models include:

- Propofol and Remifentanil synergic effects on BIS variable (surface model);
- Remifentanil effect lowering MAP and increasing CO;
- Increasing CO will increase clearance rates of Propofol, thereby increasing BIS values;

- Antagonistic effects between DP(B)/SNP and CO/MAP;

Specific features enabled by the authors as original contribution to the body of knowledge of this work are summarized hereafter.

The anesthesiologist in the loop effect is the additional bolus value given prior to surgical stimulation and has been discussed in [52]. Disturbance and bolus profiles are given as time based signals which can be added or not in the simulation.

Another feature contributed by the authors is the surgical stimulation nociceptor effect model, as experimentally identified and reported in [50]. The signal is added as a disturbance to the output of the PKPD model of Propofol and Remifentanil. In clinical practice, the incoming disturbance is anticipated by the anesthesiologist, possibly involving set-point change for depth of anesthesia variables and additional bolus infusion. For the purpose of optimal control, these actions need to be included as part of the control strategy, otherwise they may lead to sub-optimal control results as they are considered unknown disturbances acting in the system/patient [52].

For long term anesthesia, such as that in coma induced patients, bariatric surgery, organ transplant surgery and recently, in Covid-1ç patients on life support system, there is an enhanced risk for drug accumulation/trapping in slow acting tissue volumes (i.e. fat). To incorporate this feature in the simulator, a model such as described in [53] is provided to the user. This gives the possibility to choose between the classic pharmacokinetic model or a pharmacokinetic model with memory term to mimic drug trapping effects. Classical compartmental modelling theory assumes a homogeneous drug distribution as a result of nominal diffusion pattern in the tissue. However, this is not necessarily the case [51], [54]. It has been shown that slow acting compartments are more likely to have unbalanced clearance rates, therefore introducing a memory effect in the amount of drug acting on site [55]–[57], conceptually illustrated in Fig. 6.

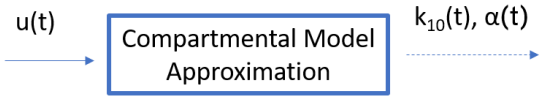

FIGURE 6. Concept of the unbalanced input $u(t)$ to clearance rate k_{10} in a heterogeneous tissue compartment with fractional kinetic factor α.

An important challenge for control design is the presence of time delay in the BIS output and in the model of hemodynamic system. This delay may vary in time. For instance, in the BIS signal, a poor signal quality may be detected in the EEG used for epoch calculation and average over time based window sample interval [58]. This artefact corrupted signal is detected through monitoring a signal quality index. If the value is below a threshold limit, then the current EEG window interval is discarded, and the BIS value from the previous valid window evaluation is provided as hypnotic level output. This introduces a time delay which may vary between 10-240 seconds [58]. The user can choose to have a delay-free BIS signal, or a constant delay value of 30 seconds, or a variable time delay within the given interval.

To summarize, Table 5 provides the reader with the overview of interactions enabled in the patient simulator. One arrow indicates a low interaction while two arrows indicates a higher interaction and the horizontal line indicated that there is no influence between the input drug and the measured output.

TABLE 5. Interactions between the inputs and outputs of the anesthesia-hemodynamic system.

Input/Output	BIS	RASS	NMB	CO	MAP
Prop	⇓	–	–	↓	↓
Remi	↓	⇓	↓	↑	↓
Atrac/Roc	–	–	⇓	–	–
Dp/Db	↑	–	–	⇑	↑
SNP	↑	–	–	↑	↑

IV. RESULTS

The Matlab-Simulink scheme of the simulator is given in Fig. 7.

Figs. 8-11 denote the results in open loop. The simulations have been performed for the artificial patient database presented in Table 1. These results indicate the interaction between the anesthesia parameters and the hemodynamic parameters. Simulations were performed by changing one input and evaluate the influence on its direct output but also on the other outputs of the system. In Fig. 8 the influence of Propofol on BIS but also on the hemodynamic variables is shown. Notice that a decrease of the Cardiac Output (CO) and Mean Arterial Pressure (MAP) is occurring. In Figs. 9-10 the influence of Dopamine and respectively SNP has been investigated and we have observed that they only have an effect on the hemodynamic variables and not on the anesthetic parameters. The influence of Remifentanil on BIS and other parameters is depicted in Fig. 11. It can be observed that Remifentanil has a small influence on the NMB as well as on the CO and MAP. Regarding the hemodynamic parameters there is a higher influence on MAP.

The addition of the hemodynamic sub-process poses high challenges on the control objective, with its delay-dominant dynamics and large interaction degree. As the cardiac output tends to increase, the hypnotic state tends to increase towards consciousness values, as the drug is cleared at faster rates from the organisms. This antagonistic situation is difficult to maintain in clinical onset. Sedation tends to lower Mean Arterial Pressure (MAP) and Cardiac Output (CO), while these need to be maintained at a safe interval value for the patient to remain in stable vital conditions.

V. DISCUSSION

The trilogy of healthcare is defined by key *M*-s: measure, model and manage. With today's computer based data records and information technology assets entering clinical practice, we witness an exponential growth of PKPD modelling for

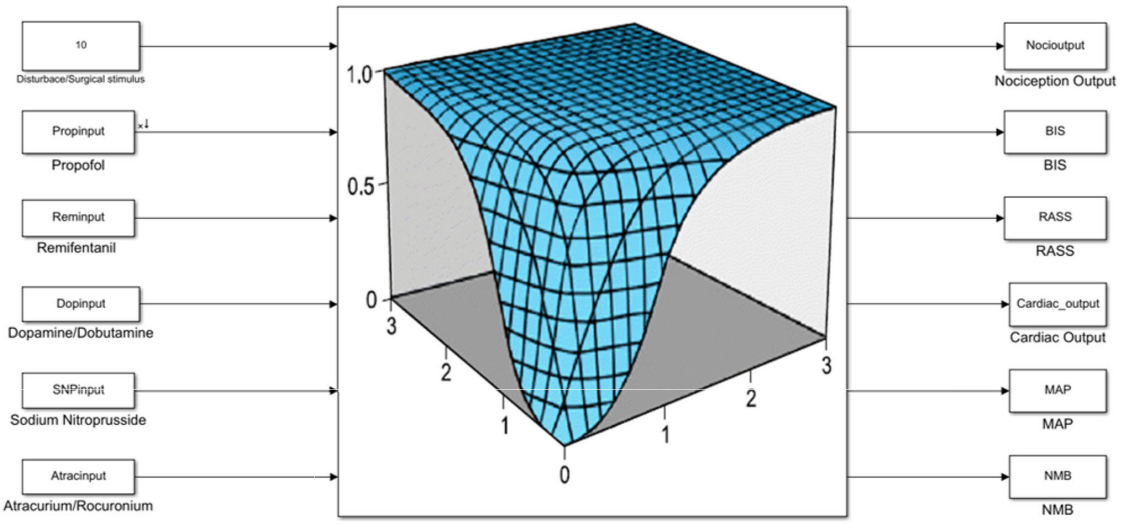

FIGURE 7. The integral structure of anesthesia-hemodynamic simulator developed in Matlab–Simulink. The simulator consists of two main subsytems: Anesthesia and Hemodynamics.

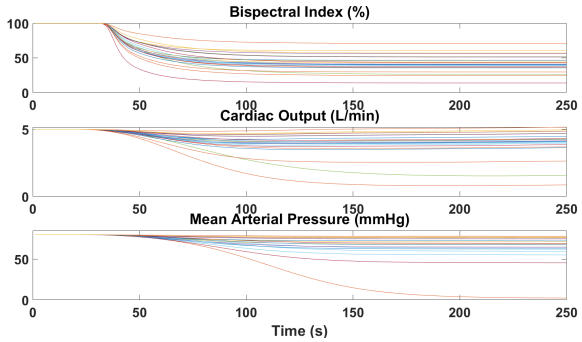

FIGURE 8. The influence of Propofol on the anesthetic and hemodynamic parameters.

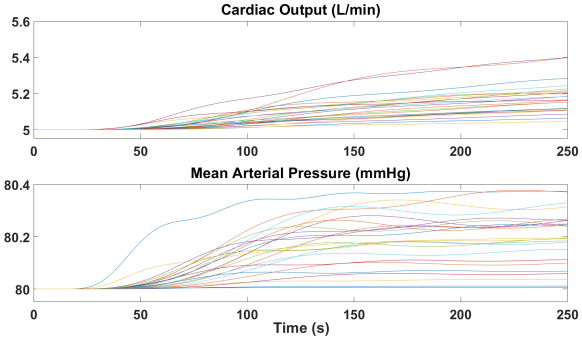

FIGURE 9. The influence of Dopamine on the hemodynamic parameters.

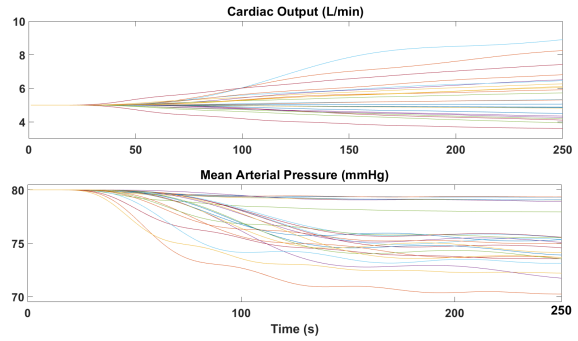

FIGURE 10. The influence of Sodium Nitroprusside on the hemodynamic parameters.

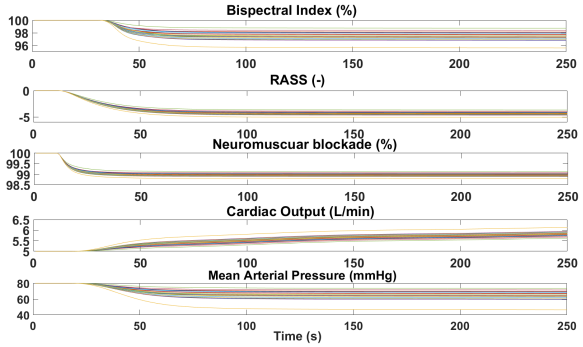

FIGURE 11. The influence of Remifentanil on the anesthetic and hemodynamic parameters.

various anesthetic and sedation drugs as comprehensively reviewed in [7]. Developments are covering both intravenous and aerosol management of depth of anesthesia [59], [60]. Influence of Propofol and Remifentanil on the hemodynamic and hypnotic states is further assessed in recent studies [61].

Recently, a novel PKPD model for Propofol has been proposed in [62], yet to be seen if applicable for optimizing closed loop control objectives. Furthermore, new evidence that brain activity modulates differently to noxious stimuli than to hypnotic states [63], enable artificial intelligence tools to predict sedation state of patients [64], [65].

The management of anesthesia moves from single drug to multi-drug co-administration, making small but essential steps forward towards a fully computerized regulatory paradigm of personalised patient services. Co-administration of Propofol and Remifentanil for anesthesia regulation has been very recently re-assessed in simulation studies [66] and in clinical trials [67].

An anesthesia patient simulator in Matlab–Simulink software platform has been proposed in [68]. This does not include the hemodynamic interaction states, nor nociceptor stimulation, and has more an educational/training purpose as they already feature closed loop control strategies. Here, in our version of the simulator, we have a series of control relevant features, which are essential to the systems and control community in order to develop computer based solutions for multi-drug management of anesthetic and hemodynamic states in presence of realistic nociceptor stimulation.

We discuss here the original contribution of our simulator through the set of features relevant for closed loop control objectives design and optimization.

BIS-controlled systems rely on epoch based estimations of EEG states as moving windows. This introduces a typical time delay of 10-30 seconds in the BIS variable. In presence of artefacts, the signal quality index decreases and epoch are discarded, the BIS value being delivered to a monitor affected by a yet longer delay interval. A study on clinical data revealed variations between 10-240 seconds [58]. This simulator includes a random assignment of values in the given interval to a variable delay block in Simulink.

Next, the Hill curves are patient-dependent and initially, when control is designed, averaged values can be used to startup simulation. There is always a model mis-match between the actual patient and the model received by the advanced model based control algorithm. It is possible the patient PD model values are to be adapted during simulation with real-time identification/estimation procedures. Two methods have been compared in [32]. However, it should be observed that during the maintenance phase, the nonlinear Hill curve sigmoidicity reduces to linear parameter dependence, as identified in [30]. The simulator has a set of PD values for each part of the multi-models included, but the model based control design could use generic values or partially modified values to introduce uncertainty in the parameters for a more realistic approach. For instance, averaged values for C_{50} and γ could be used from Table 1 while the simulator could mimic the real patient with the explicit/individualised value from the table.

Despite induction phase control strategies developed in simulation studies [8], [28], [38], [66], we reckon that this could be just as well manually managed by the anesthesiologist, for having excellent performance compared to computerized optimization. This is due to the fact that essentially linear control has been used for what is termed as the only nonlinearity present in the models: the induction phase and induction knee in the Hill curve response. Once passed this knee point, the response remains in a linear slope representation, while intra-patient variability may change the degree of the slope in time [30], [31]. The intra-patient variability is prevalent in long term surgery (e.g. bariatric, heart and lung transplant, extracorporeal membrane oxygenation, co-joint separation surgery, bionic implants/reconstruction, organ-on-a-chip surgery) or outlier patients.

On a long term perspective, there is evidence to support the claim that assumption on homogeneous distribution and uptake kinetics of drug may be too optimistic [55], [56]. As a result, drug molecules may be trapped for longer residence times than initially though [53], with recirculatory effects from liver latency processing at macromolecular and metabolic rate dynamic variability [69]. By their analogy of kinetic compartmental models to transfer function models as proposed in [26], [70], the fractal kinetics are approximated by fractional order transfer function models as those proposed in [50], [51], [71]. Their advantage is that memory effects of drug latency can be more accurately modelled, providing better models for optimal regulation of drug dosing profiles to better avoid over- and under-dosing risks. The simulator includes a pharmacokinetic model description to allow such heterogeneous diffusion effects and the user may choose freely among the classical or anomalous pharmacokinetic kinetics. This will have a visible effect on the optimisation solutions for the drug dosing profiles among advanced control strategies, if the user performs long term anesthesia simulations.

There are two limitations in the features included in this version of the simulator. Namely, the patient variability for the hemodynamic states and the PD model for the direct output of Remifentanil drug dosing rates. A PD model for analgesia as a separate output variable to be controlled is currently missing. Presently, enabled by recent commercial devices availability for objective pain level assessment, ongoing efforts in clinical trial testing [72], [73] are expected to provide the necessary data for estimating the PD model. The hemodynamic system is described as a first order plus dead time approximation of the PKPD effects. To include patient variability in this multivariable model, one may introduce variations in the model parameters: gain, time constant and dead time, as given in Table 3.

From the point of view of control, a multi-objective optimization is a reasonable assumption in the control design. However, this is a complex problem if searched for the global optimal solution at all times. It might be interesting to consider a prioritized version, in which objectives are given different levels of priority as a function of the current patient state. Such multi-objective prioritized methodology has been proposed in [74], with initial results for the anesthetic-hemodynamic system.

VI. LIMITATIONS

In the overview depicted by Fig. 1, the inputs and outputs corresponding to the anesthesia-hemodynamic system are presented. It can be noticed that there is no direct output for pain assessment and this is still a missing, yet much needed piece of the puzzle. This is a major limitation of the simulator, as data from commercial pain devices identified as PD models are unavailable yet.

Nowadays, pain is evaluated by heuristic based indexes in both awake patients (e.g. NRS) as well as in unconscious, sedated patients (e.g. RASS). Hence, there is no pharmacodynamic model for Remifentanil. In this regard, the authors developed a methodology for detecting nociceptor simulation which has been successfully validated in healthy volunteers [50] but also in post-operative ICU patients [73]. Ongoing clinical studies in unconscious patients at Ghent University Hospital will provide updates for future versions of the simulator.

VII. CONCLUSION

This open source simulator is a modest yet essential first step towards uniform design and evaluation of the drug-dosing problem in anesthesia and hemodynamic regulatory paradigm. The version provided by this paper includes the essential elements to develop suitable closed loop multivariable optimal control strategies. Despite limitations, we believe this pioneering work will create awareness in the community and enable a systematic design and evaluation of adequate solutions translatable to clinical practice. Next steps in further improving the benchmark includes the implementation of the PD model for opioid to analgesic effect identified from data in ongoing clinical studies.

APPENDIX A
MODEL PREDICTIVE CONTROL (MPC) USED TO ILLUSTRATE FEASIBILITY OF THE CLOSED LOOP

The predictive control has been shown to be closest to mimicking anesthesiologist actions during surgery [52]. We have a long-standing tradition of applying predictive control to various dynamic states in the anesthetic, which has been also used in clinical practice [75], and hemodynamic regulation problem. The used predictive control methodology has been tailored from the generic EPSAC (Extended Predictive Self-Adaptive Control) algorithm given in [28] for SISO systems, adaptive in [76] and multi-objective prioritized optimization in [74]. In this section only the essential steps in obtaining the closed loop control results given in this paper are presented. Their role is to show to the reader that a closed loop control objective is achievable with the complex simulator.

A. ESSENTIALS OF QUASI-INFINITE HORIZON MPC (QIH-MPC)

The basic principle of MPC is shown in Fig. 12, as fully described in [77]. At time t, the future states $\bar{x}$ until $t + T_p$ are predicted using the dynamic model of the system.

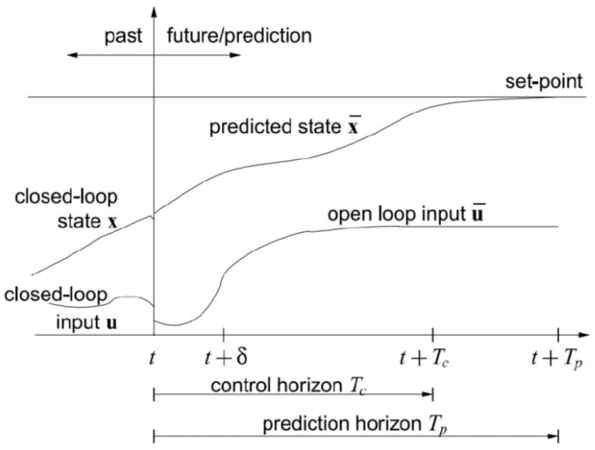

FIGURE 12. Basic Model Predictive Control Concept.

Consequently, the optimal open-loop inputs $\bar{u}$ are calculated until $t+T_c$. These optimal inputs are found by iteratively minimizing a user-defined cost function. After these calculations, the open-loop input is implemented until $t + \delta$, with δ being the sampling time. By measuring the states at $t + \delta$, a new 'initial' state is obtained. It is at this point that the scheme is shifted from t to $t + \delta$ and the whole iteration starts again, i.e. the receding horizon principle [77].

In basic MPC, the predicted states are required to be equal to the equilibrium point after the prediction horizon (terminal state equality constraint). Quasi-infinite Horizon MPC (QIHMPC) softens this constraint by demanding only that the states are within an invariant terminal region around the equilibrium point after the prediction horizon. As the terminal region is invariant, a local linear state feedback controller can be applied until the equilibrium point is reached exactly after an 'infinite' amount of time. The distance to the equilibrium point is penalized by a terminal penalty matrix included in the objective function, which is separate from the state and input weighting matrices also used in the objective function. It is important to note that the inputs are only calculated for a finite time (Tc), as the infinite 'tail' with the state feedback controller is never used in practice [77].

B. STABILITY, FEASIBILITY AND ROBUSTNESS OF QIH-MPC

The terminal penalty matrix, the local linear feedback controller and terminal region are calculated and included in the objective function because their existence and inclusion allows for a Lyapunov-argument to prove the stability of the QIH-MPC scheme. The reader can find more details on this in [77]. The following procedure for calculating these variables has been adapted from [77] and used in our initial proof of control study:

1) Calculate the Jacobian linearization (A,B) of the system at the equilibrium point
2) Check the stabilizability of the Jacobian linearization (for instance, with the Hautus-test for stabilizability).

The rest of the procedure is not applicable if the linearization is not stabilizable.

3) Find a linear state feedback matrix K such that AK is Hurwitz:

$$\begin{aligned} u &= Kx \in U, \forall x \in X \\ A_K &:= A + BK \end{aligned} \tag{20}$$

4) Solve the following Lyapunov equation to obtain the terminal penalty matrix P (with n being the number of states).

$$\begin{aligned} &Q^* = Q + K^T RK \in \Re^{n\chi n} \\ &k < -\delta_{max(A_k)}, k \in [0, \infty) \\ &(A_k + kI)^T P + P(A_k + kI) = -Q^* \end{aligned} \tag{21}$$

5) Use the state feedback matrix K to find the largest $\alpha_1 \in (0, \infty)$ such that

$$\begin{aligned} &\Omega := \{\chi \in \Re^n | \chi^T P \chi \leq \alpha_1\} \\ &K\chi \in U, \forall \chi \in \Omega_{alpha_1} \end{aligned} \tag{22}$$

6) Find the largest $\alpha \in (0, \alpha_1]$ such that

$$\begin{aligned} \dot{x} &= f(\chi, K\chi) \\ \phi(x) &:= f(\chi, K\chi) - A_k\chi \\ L_\phi &:= sup\left\{ \frac{\|\phi(\chi)\|}{\|\chi\|} \middle| \chi \in \Omega_\alpha, \chi \neq 0 \right\} \\ L_\phi &\leq \frac{k\lambda_{min}(P)}{\|P\|} \end{aligned} \tag{23}$$

with Ω_α being an invariant terminal region, $sup(\cdot)$ the supremum and $\|\cdot\|$ the Frobenius norm.

Once this procedure has successfully been completed and the results included in the controller, the stability of the QIH-MPC scheme is guaranteed if a feasible solution can be found at $t = 0$, i.e. at each sampling period that the procedure is iterated. Feasibility requires that at each time step, a solution can be found such that the states are within Ω_α after the prediction horizon (Tp). This also means robust stability is guaranteed, as long as the disturbances are small enough such that the states remain within the feasible region.

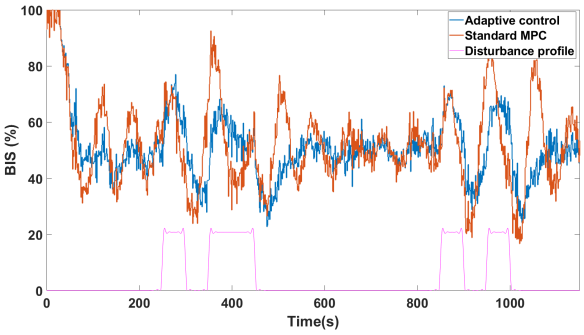

FIGURE 13. Simulated patient response for set-point tracking and disturbance rejection.

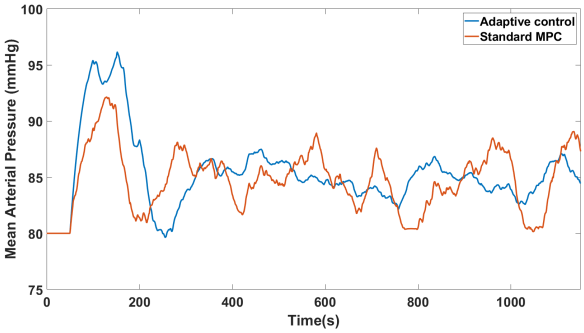

FIGURE 14. Simulated patient response for mean arterial pressure control.

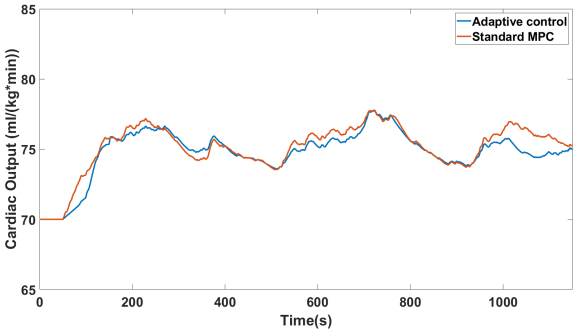

FIGURE 15. Simulated patient response for cardiac output control.

C. PRELIMINARY RESULTS

The control performance of the designed QIH-MPC controller is generally as desired, even when considering inter- and intra-patient variability as well as nociceptor stimulation and interventions by the anesthesiologist. Moreover, an adaptive control strategy [76] has been also designed and tested and the obtained results for both control strategies are shown in Fig. 13-15. Although not globally optimal, these preliminary results of the closed loop indicate that the simulator is operational and equilibrium in the anesthetic - hemodynamic states interplay can be achieved.

The results of the implemented control strategies are given in Fig. 13-15. From Fig. 13 it can be observed that when the surgical stimulus is applied (disturbance profile in this case) and the intervention of the anesthesiologist is included in the model, the controller performs satisfactory. A study on the inter-patient variability indicated that after administration of a bolus by the anesthesiologist, the BIS level as a result of patient sensitivity is varying significantly. This means that if the same surgical stimulus is then applied to all patients, patients with a lower sensitivity to drug effect will generally have a higher resulting BIS levels. Fig. 14 and Fig. 15 reveal that the initial control strategy proposed for the entire anesthetic-hemodynamic system is promising also in term of hemodynamic variables control.

However, an in-depth analysis in terms of control performance, control limitations, etc. is not the scope of this paper. A brief description of the start control theory used to design the control strategy has been given in the AppendixVII.

D. SOFTWARE

The software files are available in Matlab File Exchange platform https://nl.mathworks.com/matlabcentral/fileexchange/85208-open-source-patient-simulator

ACKNOWLEDGMENT

This benchmark is the result of many collaborations spanned across 15 years of clinical and control engineering research and involves many medical and engineer specialists. The authors would like to thank to Prof. Dr. MD. Michel MMRF Struys (UCMG, The Netherlands), Prof. Dr. MD. Patrick Wouters (UZGent, Belgium), Dr. Ir. Tom De Smet (DEMED Medical, Temse, Belgium), Em. Prof. Dr. Ir. Robin De Keyser (UGent, Belgium), and the technical implementation details executed by Ir. Frederik Kussé and Ir. Lennart Van Acker during their work on their master dissertation at Ghent University. They would also like to thank the reviewers for their positive comments and for acknowledging the importance of such a benchmark simulator to the systems and control community.

REFERENCES

[1] E. Brogi, S. Cyr, R. Kazan, F. Giunta, and T. M. Hemmerling, "Clinical performance and safety of closed-loop systems: A systematic review and meta-analysis of randomized controlled trials," *Anesthesia Analgesia*, vol. 124, no. 2, pp. 446–455, 2017.

[2] S. Bibian, C. R. Ries, M. Huzmezan, and G. Dumont, "Introduction to automated drug delivery in clinical anesthesia," *Eur. J. Control*, vol. 11, no. 6, pp. 535–557, Jan. 2005.

[3] M. M. Neckebroek, T. De Smet, and M. M. R. F. Struys, "Automated drug delivery in anesthesia," *Current Anesthesiol. Rep.*, vol. 3, no. 1, pp. 18–26, Mar. 2013.

[4] K. E. Kwok, S. L. Shah, B. A. Finegan, and G. K. Kwong, "An observational trial of a computerized drug delivery system on two patients," *IEEE Trans. Control Syst. Technol.*, vol. 5, no. 4, pp. 385–393, Jul. 1997.

[5] J. F. Biebuyck, D. A. O'Hara, D. K. Bogen, and A. Noordergraaf, "The use of computers for controlling the delivery of anesthesia," *Anesthesiology*, vol. 77, no. 3, pp. 563–581, Sep. 1992.

[6] C. Zaouter, T. Hemmerling, S. Mion, L. Leroux, A. Remy, and A. Outtara, "Feasibility of automated propofol sedation for transcatheter aortic valve implantation: A pilot study," *Anesthesia Analgesia*, vol. 125, pp. 1505–1512, Nov. 2017.

[7] C. Zaouter, A. Joosten, J. Rinehart, M. M. R. F. Struys, and T. M. Hemmerling, "Autonomous systems in anesthesia: Where do we stand in 2020? A narrative review," *Anesthesia Analgesia*, vol. 130, no. 5, pp. 1120–1132, May 2020.

[8] F. Padula, C. Ionescu, N. Latronico, M. Paltenghi, A. Visioli, and G. Vivacqua, "Inversion-based propofol dosing for intravenous induction of hypnosis," *Commun. Nonlinear Sci. Numer. Simul.*, vol. 39, pp. 481–494, Oct. 2016.

[9] M. Gorges, N. West, and S. M. Brodie, "Hemodynamic changes during closed loop induction of anesthesia," *Anesthesia Analgesia*, vol. 122, no. 3, 2016.

[10] C. L. Beck, "Modeling and control of pharmacodynamics," *Eur. J. Control*, vol. 24, pp. 33–49, Jul. 2015.

[11] R. Allen and D. Smith, "Neuro-fuzzy closed-loop control of depth of anaesthesia," *Artif. Intell. Med.*, vol. 21, nos. 1–3, pp. 185–191, Jan. 2001.

[12] W. M. Haddad, J. M. Bailey, T. Hayakawa, and N. Hovakimyan, "Neural network adaptive output feedback control for intensive care unit sedation and intraoperative anesthesia," *IEEE Trans. Neural Netw.*, vol. 18, no. 4, pp. 1049–1066, Jul. 2007.

[13] J.-S. Shieh, M. Fu, S.-J. Huang, and M.-C. Kao, "Comparison of the applicability of rule-based and self-organizing fuzzy logic controllers for sedation control of intracranial pressure pattern in a neurosurgical intensive care unit," *IEEE Trans. Biomed. Eng.*, vol. 53, no. 8, pp. 1700–1705, Aug. 2006.

[14] J.-S. Shieh, C.-Y. Dai, Y.-R. Wen, and W.-Z. Sun, "A novel fuzzy pain demand index derived from patient-controlled analgesia for postoperative pain," *IEEE Trans. Biomed. Eng.*, vol. 54, no. 12, pp. 2123–2132, Dec. 2007.

[15] A. Absalom and M. Struys, *An Overview of TCI and TIVA*. Ghent, Belgium: Academia Press, 2007.

[16] S. Goutelle, M. Maurin, F. Rougier, X. Barbaut, L. Bourguignon, M. Ducher, and P. Maire, "The hill equation: A review of its capabilities in pharmacological modelling," *Fundam. Clin. Pharmacol.*, vol. 22, no. 6, pp. 633–648, Dec. 2008.

[17] D. Gonze and W. Abou-Jaoudé, "The goodwin model: Behind the hill function," *PLoS ONE*, vol. 8, no. 8, Aug. 2013, Art. no. e69573.

[18] R. D. Miller, *Miller's Anesthesia*, 8th ed. Amsterdam, The Netherlands: Elsevier, 2015.

[19] A. Shander, G. P. Lobel, and D. M. Mathews, "Brain monitoring and the depth of anesthesia: Another goldilocks dilemma," *Anesthesia Analgesia*, vol. 126, no. 2, pp. 707–709, 2018.

[20] B. Musizza and S. Ribaric, "Monitoring the depth of anaesthesia," *Sensors*, vol. 10, no. 12, pp. 10896–10935, Dec. 2010.

[21] M. Ghita, M. Ghita, and D. Copot, "Automated drug delivery in anesthesia," in *An Overview of Computer-Guided Total Intravenous Anesthesia and Monitoring Devices–Drug Infusion Control Strategies and Analgesia Assessment in Clinical Use and Research*. Amsterdam, The Netherlands: Elsevier, 2020, pp. 7–50.

[22] B. G. Katzung and A. J. Trevor, *Basic and Clinical Pharmacology*, 13th ed. New York, NY, USA: McGraw-Hill, 2015.

[23] T. W. Schnider, C. F. Minto, P. L. Gambus, C. Andresen, D. B. Goodale, S. L. Shafer, and E. J. Youngs, "The influence of method of administration and covariates on the pharmacokinetics of propofol in adult volunteers," *Anesthesiology*, vol. 88, no. 5, pp. 1170–1182, May 1998.

[24] T. W. Schnider, C. F. Minto, S. L. Shafer, P. L. Gambus, C. Andresen, D. B. Goodale, and E. J. Youngs, "The influence of age on propofol pharmacodynamics," *Anesthesiology*, vol. 90, no. 6, pp. 1502–1516, Jun. 1999.

[25] C. F. Minto, T. W. Schnider, T. D. Egan, E. Youngs, H. J. M. Lemmens, P. L. Gambus, V. Billard, J. F. Hoke, K. H. P. More, D. J. Hermann, K. T. Muir, J. W. Mandema, and S. L. Shafer, "Influence of age and gender on the pharmacokinetics and pharmacodynamics of remifentanil: I. Model development," *Anesthesiology*, vol. 86, no. 1, pp. 10–23, 1997.

[26] K. Soltesz, J.-O. Hahn, T. Hägglund, G. A. Dumont, and J. M. Ansermino, "Individualized closed-loop control of propofol anesthesia: A preliminary study," *Biomed. Signal Process. Control*, vol. 8, no. 6, pp. 500–508, Nov. 2013.

[27] C. F. Minto, M. White, N. Morton, and G. N. Kenny, "Pharmacokinetics and pharmacodynamics of remifentanil, II. Model application," *Anesthesiology*, vol. 86, no. 1, pp. 24–33, 1997.

[28] C. M. Ionescu, R. De Keyser, B. C. Torrico, T. De Smet, M. M. Struys, and J. E. Normey-Rico, "Robust predictive control strategy applied for propofol dosing using BIS as a controlled variable during anesthesia," *IEEE Trans. Biomed. Eng.*, vol. 55, no. 9, pp. 2161–2170, Sep. 2008.

[29] D. Copot and C. M. Ionescu, "Drug delivery system for general anesthesia: Where are we?" in *Proc. IEEE Int. Conf. Syst., Man, Cybern. (SMC)*, Oct. 2014, pp. 2452–2457.

[30] C. Ionescu, J. Tenreiro Machado, R. De Keyser, J. Decruyenaere, and M. M. R. F. Struys, "Nonlinear dynamics of the patient's response to drug effect during general anesthesia," *Commun. Nonlinear Sci. Numer. Simul.*, vol. 20, no. 3, pp. 914–926, Mar. 2015.

[31] R. D. Keyser, D. Copot, and C. Ionescu, "Estimation of patient sensitivity to drug effect during propofol hypnosis," in *Proc. IEEE Int. Conf. Syst., Man, Cybern.*, Hong Kong, Oct. 2015, pp. 2487–2491.

[32] C. M. Ionescu, "A computationally efficient hill curve adaptation strategy during continuous monitoring of dose–effect relation in anaesthesia," *Nonlinear Dyn.*, vol. 92, no. 3, pp. 843–852, May 2018.

[33] S. Milne, G. Kenny, and S. Schraag, "Propofol sparing effect of remifentanil using closed loop anaesthesia," *Brit. J. Anaesthesia*, vol. 90, no. 5, pp. 623–629, 2003.

[34] Z. T. Zhusubaliyev, A. Medvedev, and M. M. Silva, "Bifurcation analysis of PID-controlled neuromuscular blockade in closed-loop anesthesia," *J. Process Control*, vol. 25, pp. 152–163, Jan. 2015.

[35] B. Weatherley, S. Williams, and E. Neill, "Pharmacokinetics, pharmacodynamics and dose-response relationships of atracurium administered iv," *Brit. J. Anaesthesia*, vol. 55, pp. 39S–45S, Mar. 1983.

[36] C. Rocha, T. Mendonça, and M. E. Silva, "Individualizing propofol dosage: A multivariate linear model approach," *J. Clin. Monitor. Comput.*, vol. 28, no. 6, pp. 525–536, Dec. 2014.

[37] C. M. Ionescu, I. Nascu, and R. De Keyser, "Lessons learned from closed loops in engineering: Towards a multivariable approach regulating depth of anaesthesia," *J. Clin. Monitor. Comput.*, vol. 28, no. 6, pp. 537–546, Dec. 2014.

[38] R. Padmanabhan, N. Meskin, C. M. Ionescu, and W. M. Haddad, "A nonovershooting tracking controller for simultaneous infusion of anesthetics and analgesics," *Biomed. Signal Process. Control*, vol. 49, pp. 375–387, Mar. 2019.

[39] C. Zaouter, T. M. Hemmerling, R. Lanchon, E. Valoti, A. Remy, S. Leuillet, and A. Ouattara, "The feasibility of a completely automated total IV anesthesia drug delivery system for cardiac surgery," *Anesthesia Analgesia*, vol. 123, no. 4, pp. 885–893, Oct. 2016.

[40] R. E. Kates and C. V. Leier, "Dobutamine pharmacokinetics in severe heart failure," *Clin. Pharmacol. Therapeutics*, vol. 24, no. 5, pp. 537–541, Nov. 1978.

[41] L. Mahoney, G. Shah, D. Crook, H. Rojas-Anaya, and H. Rabe, "A literature review of the pharmacokinetics and pharmacodynamics of dobutamine in neonates," *Pediatric Cardiol.*, vol. 37, no. 1, pp. 14–23, Jan. 2016.

[42] W. Habre, N. Disma, K. Virag, K. Becke, T. G. Hansen, M. Jöhr, B. Leva, N. S. Morton, P. M. Vermeulen, M. Zielinska, K. Boda, and F. Veyckemans, "Incidence of severe critical events in paediatric anaesthesia (APRICOT): A prospective multicentre observational study in 261 hospitals in Europe," *Lancet Respiratory Med.*, vol. 5, no. 5, pp. 425–1412, 2017.

[43] S. Isaka and A. V. Sebald, "Control strategies for arterial blood pressure regulation," *IEEE Trans. Biomed. Eng.*, vol. 40, no. 4, pp. 353–363, Apr. 1993.

[44] G. I. Voss, P. G. Katona, and H. J. Chizeck, "Adaptive multivarable drug delivery: Control of artenal pressure and cardiac output in anesthetized dogs," *IEEE Trans. Biomed. Eng.*, vol. BME-34, no. 8, pp. 617–623, Aug. 1987.

[45] R. Rao, C. Palerm, B. Aufderheide, and W. Bequette, "Experimental studies on automated regulation of hemodynamic variables," *IEEE Eng. Med. Biol. Mag.*, vol. 20, pp. 24–38, Aug. 2000.

[46] R. R. Rao, B. Aufderheide, and B. W. Bequette, "Experimental studies on multiple-model predictive control for automated regulation of hemodynamic variables," *IEEE Trans. Biomed. Eng.*, vol. 50, no. 3, pp. 277–288, Mar. 2003.

[47] C. Zaouter, T. M. Hemmerling, R. Lanchon, E. Valoti, A. Remy, S. Leuillet, and A. Ouattara, "The feasibility of a completely automated total IV anesthesia drug delivery system for cardiac surgery," *Anesthesia Analgesia*, vol. 123, no. 4, pp. 885–893, Oct. 2016.

[48] J. F. Standing, G. B. Hammer, W. J. Sam, and D. R. Drover, "Pharmacokinetic–pharmacodynamic modeling of the hypotensive effect of remifentanil in infants undergoing cranioplasty," *Pediatric Anesthesia*, vol. 20, no. 1, pp. 7–18, Jan. 2010.

[49] M. M. R. F. Struys, T. De Smet, S. Greenwald, A. R. Absalom, S. Bingé, and E. P. Mortier, "Performance evaluation of two published closed-loop control systems using bispectral index monitoring," *Anesthesiology*, vol. 100, no. 3, pp. 640–647, Mar. 2004.

[50] D. Copot and C. Ionescu, "Models for nociception stimulation and memory effects in awake and aware healthy individuals," *IEEE Trans. Biomed. Eng.*, vol. 66, no. 3, pp. 718–726, Mar. 2019.

[51] C. M. Ionescu, A. Lopes, D. Copot, J. T. Machado, and J. H. T. Bates, "The role of fractional calculus in modeling biological phenomena: A review," *Commun. Nonlinear Sci. Numer. Simul.*, vol. 51, pp. 141–159, Oct. 2017.

[52] C. M. Ionescu, D. Copot, and R. De Keyser, "Anesthesiologist in the loop and predictive algorithm to maintain hypnosis while mimicking surgical disturbance," *IFAC-PapersOnLine*, vol. 50, no. 1, pp. 15080–15085, Jul. 2017.

[53] D. Copot, R. L. Magin, R. De Keyser, and C. Ionescu, "Data-driven modelling of drug tissue trapping using anomalous kinetics," *Chaos, Solitons Fractals*, vol. 102, pp. 441–446, Sep. 2017.

[54] D. Sierociuk, T. Skovranek, M. Macias, I. Podlubny, I. Petras, A. Dwielinski, and P. Ziubinski, "Diffusion process modeling by using fractional-order models," *Appl. Math. Comput.*, vol. 257, pp. 2–11, Apr. 2015.

[55] M. Weiss, "Comparison of distributed and compartmental models of drug disposition: Assessment of tissue uptake kinetics," *J. Pharmacokinetics Pharmacodynamics*, vol. 43, no. 5, pp. 505–512, Oct. 2016.

[56] P. Sopasakis, H. Sarimveis, P. Macheras, and A. Dokoumetzidis, "Fractional calculus in pharmacokinetics," *J. Pharmacokinetics Pharmacodynamics*, vol. 45, no. 1, pp. 107–125, Feb. 2018.

[57] M. Hennion and E. Hanert, "How to avoid unbounded drug accumulation with fractional pharmacokinetics," *J. Pharmacokinetics Pharmacodynamics*, vol. 40, no. 6, pp. 691–700, Dec. 2013.

[58] C. M. Ionescu, R. Hodrea, and R. De Keyser, "Variable time-delay estimation for anesthesia control during intensive care," *IEEE Trans. Biomed. Eng.*, vol. 58, no. 2, pp. 363–369, Feb. 2011.

[59] M. H. Kuizenga, P. J. Colin, K. M. E. M. Reyntjens, D. J. Touw, H. Nalbat, F. H. Knotnerus, H. E. M. Vereecke, and M. M. R. F. Struys, "Population pharmacodynamics of propofol and sevoflurane in healthy volunteers using a clinical score and the patient state index," *Anesthesiology*, vol. 131, no. 6, pp. 1223–1238, Dec. 2019.

[60] M. A. S. Weerink, C. R. M. Barends, E. R. R. Muskiet, K. M. E. M. Reyntjens, F. H. Knotnerus, M. Oostra, J. F. P. van Bocxlaer, M. M. R. F. Struys, and P. J. Colin, "Pharmacodynamic interaction of remifentanil and dexmedetomidine on depth of sedation and tolerance of laryngoscopy," *Anesthesiology*, vol. 131, no. 5, pp. 1004–1017, Nov. 2019.

[61] J. P. van den Berg, A. R. Absalom, A. M. Venema, A. F. Kalmar, K. Van Amsterdam, L. N. Hannivoort, J. H. Proost, S. Meier, T. W. L. Scheeren, M. M. R. F. Struys, and H. E. M. Vereecke, "Comparison of haemodynamic- and electroencephalographic-monitored effects evoked by four combinations of effect-site concentrations of propofol and remifentanil, yielding a predicted tolerance to laryngoscopy of 90%," *J. Clin. Monitor. Comput.*, Jun. 2020, doi: 10.1007/s10877-020-00540-9.

[62] D. J. Eleveld, P. Colin, A. R. Absalom, and M. M. R. F. Struys, "Pharmacokinetic–pharmacodynamic model for propofol for broad application in anaesthesia and sedation," *Brit. J. Anaesthesia*, vol. 120, no. 5, pp. 942–959, May 2018.

[63] L. Tiemann, V. D. Hohn, S. Ta Dinh, E. S. May, M. M. Nickel, J. Gross, and M. Ploner, "Distinct patterns of brain activity mediate perceptual and motor and autonomic responses to noxious stimuli," *Nature Commun.*, vol. 9, no. 1, p. 4487, Dec. 2018.

[64] S. Belur Nagaraj, S. M. Ramaswamy, M. A. S. Weerink, and M. M. R. F. Struys, "Predicting deep hypnotic state from sleep brain rhythms using deep learning: A data-repurposing approach," *Anesthesia Analgesia*, vol. 130, no. 5, pp. 1211–1221, May 2020.

[65] G. Wang, Z. Liu, Y. Feng, J. Li, H. Dong, D. Wang, J. Li, N. Yan, T. Liu, and X. Yan, "Monitoring the depth of anesthesia through the use of cerebral hemodynamic measurements based on sample entropy algorithm," *IEEE Trans. Biomed. Eng.*, vol. 67, no. 3, pp. 807–816, Mar. 2020.

[66] L. Merigo, F. Padula, N. Latronico, M. Paltenghi, and A. Visioli, "Optimized PID control of propofol and remifentanil coadministration for general anesthesia," *Commun. Nonlinear Sci. Numer. Simul.*, vol. 72, pp. 194–212, Jun. 2019.

[67] M. Neckebroek, J.-W.-H. L. Boldingh, T. De Smet, and M. M. R. F. Struys, "Influence of remifentanil on the control performance of the bispectral index controlled Bayesian-based closed-loop system for propofol administration," *Anesthesia Analgesia*, vol. 130, no. 6, pp. 1661–1669, Jun. 2020.

[68] M. Fang, Y. Tao, and Y. Wang, "An enriched simulation environment for evaluation of closed-loop anesthesia," *J. Clin. Monitor. Comput.*, vol. 28, no. 1, pp. 13–26, Feb. 2014.

[69] H. Cordes, C. Thiel, V. Baier, L. M. Blank, and L. Kuepfer, "Integration of genome-scale metabolic networks into whole-body PBPK models shows phenotype-specific cases of drug-induced metabolic perturbation," *NPJ Syst. Biol. Appl.*, vol. 4, no. 1, p. 11, Dec. 2018.

[70] K. van Heusden, K. Soltesz, E. Cooke, S. Brodie, N. West, M. Gorges, J. M. Ansermino, and G. A. Dumont, "Optimizing robust PID control of propofol anesthesia for children: Design and clinical evaluation," *IEEE Trans. Biomed. Eng.*, vol. 66, no. 10, pp. 2918–2923, Oct. 2019.

[71] I. Assadi, A. Charef, D. Copot, R. De Keyser, T. Bensouici, and C. Ionescu, "Evaluation of respiratory properties by means of fractional order models," *Biomed. Signal Process. Control*, vol. 34, pp. 206–213, Apr. 2017.

[72] D. Copot, *Automated Drug Delivery in Anesthesia*. Amsterdam, The Netherlands: Elsevier, 2020.

[73] M. Neckebroek, M. Ghita, M. Ghita, D. Copot, and C. M. Ionescu, "Pain detection with bioimpedance methodology from 3-dimensional exploration of nociception in a postoperative observational trial," *J. Clin. Med.*, vol. 9, no. 3, p. 684, Mar. 2020.

[74] C. Ionescu, R. Alfredo Cajo Diaz, S. Zhao, M. Ghita, M. Ghita, and D. Copot, "A low computational cost, prioritized, multi-objective optimization procedure for predictive control towards cyber physical systems," *IEEE Access*, vol. 8, pp. 128152–128166, 2020.
[75] M. Neckebroek, C. M. Ionescu, K. van Amsterdam, T. De Smet, P. De Baets, J. Decruyenaere, R. De Keyser, and M. M. R. F. Struys, "A comparison of propofol-to-BIS post-operative intensive care sedation by means of target controlled infusion, Bayesian-based and predictive control methods: An observational, open-label pilot study," *J. Clin. Monitor. Comput.*, vol. 33, no. 4, pp. 675–686, Aug. 2019, doi: 10.1007/s10877-018-0208-2.
[76] J. Niño, R. De Keyser, S. Syafiie, C. Ionescu, and M. Struys, "EPSAC-controlled anesthesia with online gain adaptation," *Int. J. Adapt. Control Signal Process.*, vol. 23, no. 5, pp. 455–471, Nov. 2008.
[77] H. Chen and F. Allgöwer, "A quasi-infinite horizon nonlinear model predictive control scheme with guaranteed stability," *Automatica*, vol. 34, no. 10, pp. 1205–1218, 1998.

CLARA M. IONESCU (Senior Member, IEEE) received the M.Sc. degree in industrial informatics and automation from the Dunarea de Jos University of Galati, Romania, in 2003, and the Ph.D. degree from Ghent University, Belgium, in 2009, with a focus on modeling the human respiratory system with fractional order models for diagnosis purposes. Since October 2016, she has been a Professor with Ghent University, teaching Computer Control of Industrial Processes within the Control and Automation Master Program. She is currently working on the application of generic control algorithms (fractional, predictive, and PID-type) to dynamic processes in various application fields. From 2011 to 2016, she was a recipient of the Prestigious Flanders Research Fund Grant for postdoctoral fellows at Ghent University.

MARTINE NECKEBROEK received the master's degree in algology. She is currently pursuing the Ph.D. degree with Ghent University. She was an Anesthesiologist with the Hospital Aalst-Asse-Ninove, for eight years, with applications in anesthesiology, emergency medicine, and intensive care. She followed a 16 years specialization trajectory in the field of anesthesiology. Since 2006, she has been an Anesthesiologist with the Ghent University Hospital, with expertise in pediatric anesthesia, difficult airway risk patients, and intensive care. She is also the Vice-Director of the Department of Anesthesiology, Ghent University Hospital. She is also a Principal Investigator in clinical trials for analgesia modeling. Her research interest includes automated anesthesia with computer-based optimization algorithms. She is also a Principal Investigator in clinical trials for analgesia modeling, enrolled for doctoral degree with Ghent University.

MIHAELA GHITA (Graduate Student Member, IEEE) received the M.Sc. degree in medical informatics from the Politehnica University of Bucharest, Romania, in 2018. She is currently pursuing the Ph.D. degree with Ghent University, Belgium. Her research interests include modeling and control of drug delivery systems. She was awarded the Best Paper Young Author Award at 2019 IEEESAMI Conference in Herlany, Slovakia, for the research related to her Master Thesis work. She was a recipient of the prestigious Ph.D. Scholarship from the Flanders Research Foundation, Belgium.

DANA COPOT (Member, IEEE) received the M.Sc. degree in chemical engineering from Gheorghe Asachi Politechnica University, Iasi, Romania, in 2012, and the Ph.D. degree from Ghent University, in 2018, with a focus on modeling diffusion mechanisms in biological tissues. Her research interest includes predictive control of drug delivery systems. In 2017, she won the "Best Paper Award" at the IEEE International Conference on Intelligent Engineering Systems. She was a recipient of the Prestigious Flanders Research Foundation Grant for postdoctoral fellows at Ghent University.